

# Efficient Study of Substrate Integrated Waveguide Devices

J. Hajri, H. Hrizi, N. Sboui, H. Baudrand

**Abstract**—This paper presents a study of SIW circuits (Substrate Integrated Waveguide) with a rigorous and fast original approach based on Iterative process (WCIP). The theoretical suggested study is validated by the simulation of two different examples of SIW circuits. The obtained results are in good agreement with those of measurement and with software HFSS.

**Keywords**—Convergence study, HFSS, Modal decomposition, SIW Circuits, WCIP Method.

## I. INTRODUCTION

SIW circuits are considered quasi3D (2,5D) metal-dielectric circuits. They have a high level of integration circuits, the metal and dielectric losses moderated and the precision of manufacturing for microwave applications [1]-[3]. The architecture of these structures consists in adding to the planar circuits a network of metallic via-hole integrated in the dielectric layer. The via-holes replace electric side walls as in the case of classical waveguide.

In this paper, we propose a rigorous method of SIW circuits, based on a new iterative process. The Principle of WCIP method is based on the recurrent relation of the transverse incident-reflected waves between the two domains [4]-[7]. Transmission and reflection coefficients are presented and compared with measurements and with HFSS software (FEM method); then we evaluate the performance of the new method by comparing with HFSS, concerning the error and the simulation time.

## II. THEORY

SIW circuits presented in Fig. 1 are constituted by a dielectric substrate placed between two parallel metal planes (top and bottom), it contains a network of metallic via-holes, forming the waveguide, iris filters, filter cavity ...

On the one hand, these structures are planar, thus there are two groups of modes: TM with components ( $E_z$ ,  $H_x$  and  $H_y$ ) and TE with components ( $H_z$ ,  $E_x$  and  $E_y$ ). On the other hand, the lateral electrical plans (as in the rectangular waveguides) are replaced by a network of metallic via-hole. Which stops

the propagation of modes; who have the current lines which are perpendicular to the metallic via-holes ( $E_x, E_y$ ). Thereafter, among the two groups only TM modes satisfy the boundary conditions [1], [7], and the electric fields admits only one component, according to  $Z_z$  (the tangential components with the plan ( $X, Y$ ) are negligible). Thus the boundary conditions on the metal planes are automatically guarantees and only the conditions on the boundaries of metal vias are to study.

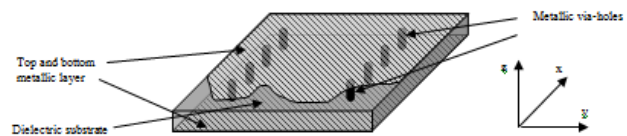


Fig. 1 SIW geometry

### A. Spatial Operator

The metallic via-hole is localized in the propagation medium, and is directed along  $z$ . At any point, we define the incident and reflected waves as a linear combination of the vertical components of the electromagnetic field, as in (1):

$$\begin{cases} A_z = \frac{1}{2\sqrt{z_0}}(E_z + z_0 J_z) \\ B_z = \frac{1}{2\sqrt{z_0}}(E_z - z_0 J_z) \end{cases} \quad (1)$$

where  $z_0$  is a normalization quantity which has an impedance dimensions.

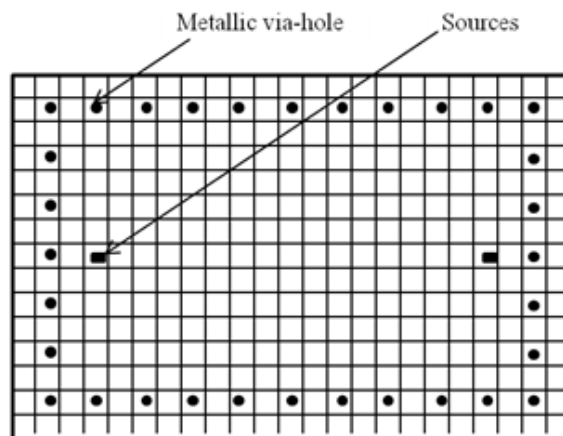


Fig. 2 Mesh of Substrate Integrated Cavity

For example, the integrated substrate cavity shown in Fig. 2

J.Hajri is with the Sciences Faculty of Tunis, University of Tunis El Manar, Tunis 2092, Tunisie (corresponding author to provide phone: +216.22696726; e-mail: hajri.jamel83@gmail.com).

H. Hrizi is with the Sciences Faculty of Tunis, University of Tunis El Manar 2092 Tunis, Tunisie.

N. Sboui is with Riyadh College of Technology, Abdulrahman bin Hassan Algosaibi, Salah Ad Din, Riyadh 12433, Saudi Arabia

H. Baudrand is with University of Toulouse, INPT, UPS, LAPLACE, ENSEEIHT, CNRS 2, Rue Charles Camichel, B.P. 7122, CP 31071 Toulouse, Cedex 7, France.

contains three sub domains: sources cells, cells with metallic via-hole and cells without metallic via-hole. Each of the three sub domain is defined by a specific matrix with same size:

$$[H_\delta]_{N_x, N_y} = \begin{cases} 1 & \text{on the Domain "}\delta\text{"} \\ 0 & \text{elsewhere} \end{cases}$$

where  $\delta$  is source, metallic via-hole and without metallic via-hole.  $N_x$  is the number of cells according to  $ox$ , and  $N_y$  is the number of cells according to  $oy$ .

In the next study, the boundary conditions for each point of the structure are presented by a spatial coefficient.

The operator  $\Omega$  describes the relations between the incident waves  $A_z$  and the reflected waves  $B_z$  in the spatial domain as in (2). Its calculation requires appropriate boundary conditions.

$$A_z(i, j) = [\Omega(i, j)]B_z(i, j) + \mathbf{A}_0 \quad (2)$$

With  $(i, j)$  are the coordinates of the cell in the total structure, and  $\mathbf{A}_0$  is the excitation defined on the source domain. The boundary conditions in all the sub domains are given by (3):

$$\begin{cases} \text{metallic via - hole } H_v : E_z = 0, J_z \neq 0 \\ \text{without via - hole } H_{nv} : E_z \neq 0, J_z = 0 \\ \text{source } H_s : E_z = E_0, J_z = J_0 = \frac{E_0}{z_0} \end{cases} \quad (3)$$

From (1) and (3), we determine the relationship between the incidents and reflected waves, as in (4):

$$\begin{cases} H_v \Rightarrow A_z^{k+1} = -B_z^k \\ H_{nv} \Rightarrow A_z^{k+1} = B_z^k \\ A_z^{k+1} = 0 \cdot B_z^{k+1} + A_0 \end{cases} \quad (4)$$

where 'k' is the iteration number.

The resulting expression for the spatial operator in (2) is given by (5):

$$\Omega = 0.H_s + H_{nv} - H_v \quad (5)$$

### B. Spectral Study

The spectral operator links the waves  $A$  and  $B$  in the spectral domain, as in (6):

$$[\tilde{B}] = [\Gamma] \cdot [\tilde{A}] \quad (6)$$

The transition between the spectral and spatial domains is ensured by a Fast Transformation in Mode using a 2D-FFT.

To solve the problem of diffraction we assume that the structure is 2D-periodic. We consider a bi-periodic array in

SIW technology presented in Fig. 3 (a)  $D_x$ , and  $D_y$  are the dimensions of the structure according to  $Ox$  and  $Oy$  axes.

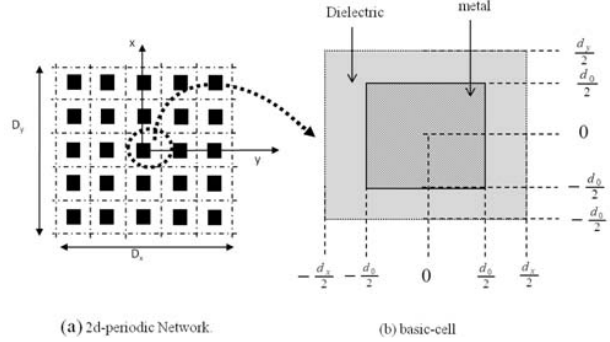


Fig. 3 Bottom view of the SIW circuit with square metallic via-hole.

$d_x$  and  $d_y$  are the periods according to  $(Ox)$  and  $(Oy)$  axes.  $d_0$  is the effective domain of the metal in the basic cell presented in Fig. 3 (b);  $h$  is the thickness of dielectric. We consider the component  $E_z$  of the electric field. The Helmholtz equation then becomes (7):

$$(\Delta_T + k^2)E_z = j\omega\mu J_z \quad (7)$$

where  $\Delta_T$  is the transverse Laplace operator and  $J = H \times \vec{n}$  is the vector of magnetic density current, and  $\vec{n}$  is normal vector.

The interaction between the periodic metallic via-holes is governed by the Floquet-Bloch theorem, and the electromagnetic fields can be decomposed on the modal base:

$$|f_{pq,mn}\rangle = a_{pq,mn} \cdot e^{j\alpha_p x} \cdot e^{j\beta_q y} \cdot e^{j\frac{2\pi m}{d_x} x} \cdot e^{j\frac{2\pi n}{d_y} y}$$

with  $\alpha_p$  and  $\beta_q$  are Floquet-Bloch states, given by:

$$\alpha_p = \frac{2\pi p}{D_x}, \beta_q = \frac{2\pi q}{D_y}$$

$a_{pq,mn} = \langle f_{pq,mn} | f_{pq,mn} \rangle$  are the ponderations of the components  $f_{pq,mn}$ .

The electric field and the current density can be written as a sum of Floquet-Bloch states, as in (9):

$$\begin{cases} E = \sum_{pq} |f_{pq}\rangle \tilde{E}_{pq} \langle f_{pq}| \\ J = \sum_{pq} |f_{pq}\rangle \tilde{J}_{pq} \langle f_{pq}| \end{cases} \quad (9)$$

We consider that the main cell is located in the center of the structure. And the indices  $p$  and  $q$  vary as:

$$-\frac{N_x}{2} \leq p \leq \frac{N_x}{2} - 1 \text{ and } -\frac{N_y}{2} \leq q \leq \frac{N_y}{2} - 1$$

The projection of the operator  $\Delta_T$  in (7), on the basis  $f_{pq,mn}$  gives (10):

$$\Delta_T f_{pq,mn} = -\left(\alpha_p + \frac{2\pi p}{d_x}\right)^2 - \left(\beta_q + \frac{2\pi q}{d_y}\right)^2 \quad (10)$$

The electric field vector and the current density on metal sub-domain are given by (11):

$$\begin{cases} E_{pq} = \langle \tilde{E}_{pq} | h_m \rangle \\ J_{pq} = \langle \tilde{J}_{pq} | h_m \rangle \end{cases} \quad (11)$$

With  $h_m$  is the projection operator in metal sub-domain in the base cell defined as:

$$h_m = \begin{cases} 1 & \text{si } (x, y) \in \left[-\frac{d_0}{2}, \frac{d_0}{2}\right] \times \left[-\frac{d_0}{2}, \frac{d_0}{2}\right] \\ 0 & \text{elsewhere} \end{cases}$$

We define the operator  $z_{pq}$  connecting the spectral components  $J_{pq}$  and  $E_{pq}$ , (12):

$$E_{pq} = z_{pq} J_{pq} \quad (12)$$

We decompose the impedance operator  $z$  on the modal base  $\langle f_{pq} |$ :

$$z = \sum_{p,q} |f_{pq}\rangle z_{pq} \langle f_{pq}| \quad (13)$$

We can decompose  $z$  on the local base:  $\langle f_{pq} f_{mn} |$ , as in (14):

$$z_{pq} = \sum_{m,n} |f_{pq} f_{mn}\rangle z_{pq,mn} \langle f_{pq} f_{mn}| \quad (14)$$

From (7), (10), (12), (14); we can write the impedance operator in the metal sub-domain as in (15):

$$z_{pq} = \sum_{m,n} \langle H_m | f_{pq} f_{mn} \rangle j\omega\mu \frac{1}{k^2 - \alpha_{p,m}^2 - \beta_{q,n}^2} \langle f_{pq} f_{mn} | H_m \rangle \quad (15)$$

$$\text{with } \alpha_{p,m} = \alpha_p + \frac{2\pi m}{d_x} \text{ and } \beta_{q,n} = \beta_q + \frac{2\pi n}{d_y}$$

Therefore

$$z_{pq} = \sum_{mn} j\omega\mu \frac{\left| \langle H_m f_{pq} f_{mn} \rangle \right|^2}{\gamma_{pq}} \quad (16)$$

with  $H_m = \frac{1}{\sqrt{s}} h_m$  and  $s$  is the cross section of metallic via-hole and  $\gamma_{pq} = (k^2 - \alpha_{p,m}^2 - \beta_{q,n}^2)$  is the propagation constant.

In the case of a structure closed by a ground plane at a distance  $h$ ,  $\Gamma_{pq}$  is given by (17):

$$\Gamma_{pq} = \frac{z_0 - z_{pq} \coth(\gamma_{pq} h)}{z_0 + z_{pq} \coth(\gamma_{pq} h)} \quad (17)$$

The calculation of output parameters is made after the convergence of the result. The distribution of the electric field and the current is given (18):

$$\begin{cases} E_z(i, j) = \sqrt{Z_0} (A_z(i, j) + B_z(i, j)) \\ J_z(i, j) = \frac{1}{\sqrt{Z_0}} (A_z(i, j) - B_z(i, j)) \end{cases} \quad (18)$$

The matrix  $S$  is given by:

$$[S] = \begin{bmatrix} [I_d] - z_0[Y] \\ [I_d] - z_0[Y] \end{bmatrix} \quad (19)$$

with  $I_d$  is the identity matrix.

### C. Application: Integrated Substrate Cavity

In order to validate the presented theoretical approach, we consider a substrate integrated cavity. The structure presented in Fig. 4 is a single substrate integrated cavity [8], the lateral walls are realized by rows of metallic via-holes through a substrate of relative dielectric constant equal to 3.58, and the thickness is 0.787mm. The total structure dimensions are  $15.17 \times 24 \text{ mm}$ . The metallic via-holes have the same diameter:  $d_0 = 0.2 \text{ mm}$  and with a period  $p = 2 \text{ mm}$ .

Fig. 5 presents the convergence curves of the reflection and transmission coefficients at a frequency equal to 10 GHz, with a ripple rate of from 200 iterations.

Also we are studied the convergence as function of the number of modes (M and N). Then the modes which have negligible amplitude will be excluded from calculation. The curves in Fig. 6 (a) present the behavior of the reflexion coefficient (S11) depending on the number of modes (M, N). Fig. 6 (b) represents the convergence curve of resonant frequency of the cavity depending on the number of modes

(M, N). We observe that the convergence start from  $M = N = 30$ . This study shows that it is unnecessary to take a number of modes higher than 30.

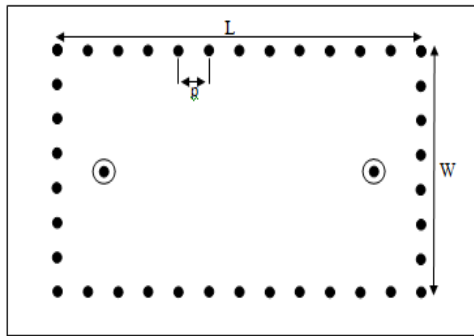


Fig. 4 Substrate integrated cavity

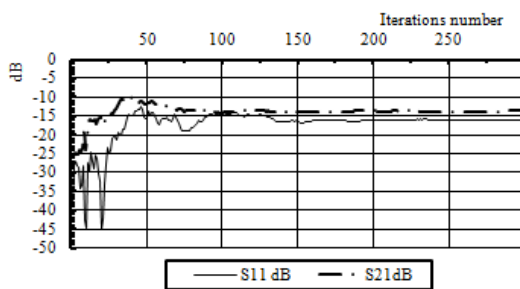


Fig. 5 Convergence curves of S-parameters as a function of iterations

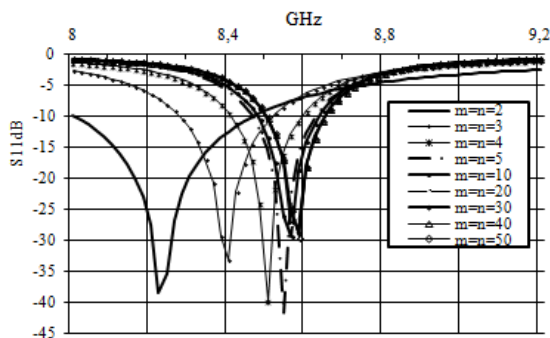


Fig. 6 (a) S11 parameters for different number of the modes

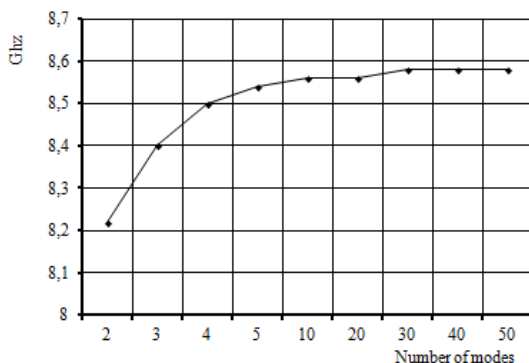


Fig. 6 (b) Resonance frequency depending of the number of modes (M,N)

The results obtained with the WCIP method are compared with a powerful analysis which use the finite element method FEM (commercial software HFSS), and also compared with measurements recently published in the literature [8].

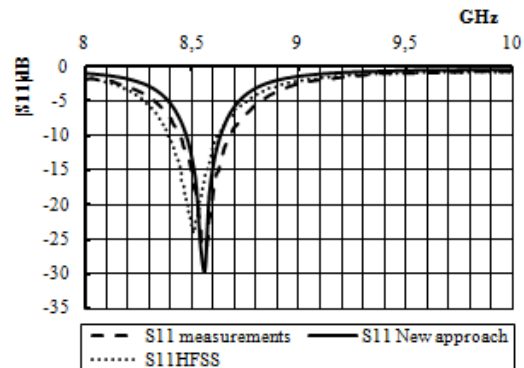


Fig. 7 (a) Reflection coefficient S11

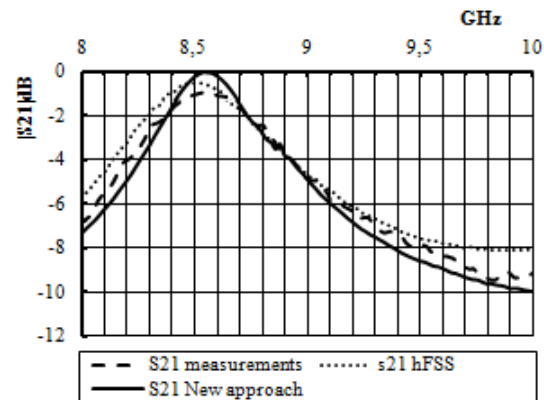


Fig. 7 (b) Transmission coefficient S21

Figs. 7 (a) and (b) show the coefficient of transmission and reflection in the frequency range: 8-10GHz. They are in good agreement with measurements and the same with simulations obtained by HFSS software. The HFSS software present a frequency shift of 55MHz, this shift is close to zero for our method.

### III. CONCLUSION

In this paper, a new formulation of iterative method with longitudinal waves was proposed. The numerical complexity is studied and compared with commercial software HFSS. Stability and convergence of the new approach are provided. The accuracy and quickness of the results are guaranteed. Our method is efficient and recommended for the analysis of structures in integrated substrate technology which have large sizes.

### REFERENCES

- [1] T. Castellano, O. Losito, L. Mescia, M. A. Chiapperino, G. Venanzoni, D. Mencarelli, G. Angeloni, C. Renghini, P. Carta, and F. Prudeniano, "Feasibility investigation of low cost substrate integrated waveguide

- (SIW) directional couplers," Progress In Electromagnetics Research B, Vol. 59, pp. 31-44, 2014.
- [2] R.Bochra, F.Mohammed, JunwuTao, "analysis of s-band substrate integrated waveguide power divider, circulator and coupler", IJCSIEA, international journal of computer science, engineering and applications, vol. 4, no.2, pp.1-14, apr. 2014.
  - [3] H. Kang, S. Lim, "Electrically small dual-band substrate-integrated-waveguide Electrically small dual-band substrate-integrated-waveguide antennas with fixed low-frequency and tunable high-frequency bands", IEICE Electronics Express, Vol.11, No.5-8,2014.
  - [4] H. Hrizi, N. Sboui, "Reducing the Numerical Calculation in the Wave Iterative Method by Image Processing Techniques", Applied Computational Electromagnetic Society journal, Vol.27 Num. 6, 2012.
  - [5] N. Sboui, A. Gharsallah, H. Baudrand, A. Gharbi, "Global Modeling of Periodic Structure in Coplanar Wave Guide", Microwave and Opt. Techno. Lett Vol. 43, No. 2 October pp: 157-160,2004.
  - [6] N.Sboui, A. Gharsallah, A. Gharbi and H. Baudrand, "global modeling of microwave active circuits by an efficient iterative procedure," international journal of rf and microwave computer-aided engineering, vol. 148, no. 3, pp. 209-212,2001.
  - [7] 7. N. Sboui, A. Gharsallah, H. Baudrand, A. Gharbi, "Modélisation Electromagnétique Globale des structures Inhomogènes", OHD2007 5-8 Septembre 2007 Valence FRANCE.
  - [8] G. Amendola, E. Arnieri, and L. Boccia, "analysis of lossy siw structures based on the parallel plates waveguide green's function", progress in electromagnetics research c, vol. 33, 157-169, 2012.